2013-07-23

Mariana Forearc Crust CORK Pressure Data: Observations and Implications

Keri A. Vinas
University of Miami, vinas.keri@gmail.com

UNIVERSITY OF MIAMI

MARIANA FOREARC CRUST CORK PRESSURE DATA: OBSERVATIONS AND IMPLICATIONS

By

Keri A.Vinas

A THESIS

Submitted to the Faculty
of the University of Miami
in partial fulfillment of the requirements for
the degree of Master of Science

Coral Gables, Florida

August 2013

UNIVERSITY OF MIAMI

A thesis submitted in partial fulfillment of
the requirements for the degree of
Master of Science

MARIANA FOREARC CRUST CORK PRESSURE DATA: OBSERVATIONS AND IMPLICATIONS

Keri A. Vinas

Approved:

_____ Keir Becker, Ph.D. Professor of Marine Geology and Geophysics	_____ M. Brian Blake, Ph.D. Dean of the Graduate School
_____ Guoqing Lin, Ph.D. Assistant Professor of Marine Geology and Geophysics	_____ John Van Leer, Ph.D. Associate Professor of Meteorology and Physical Oceanography

VINAS, KERI A. (M.S., Marine Geology and Geophysics)
Mariana Forearc Crust CORK Pressure Data: Observations and Implications (August 2013)

Abstract of a thesis at the University of Miami.

Thesis supervised by Professor Keir Becker.
No. of pages in text. (36)

Ocean Drilling Program (ODP) Leg 195 Hole 1200C was drilled and instrumented with a CORK subsurface borehole observatory in March of 2001. This CORK is located in the Mariana forearc region, 85 km away from the Mariana trench at 266 meters below seafloor and is installed atop South Chamorro Seamount, a blueschist serpentine mud volcano. The observatory is instrumented with pressure transducers, temperature thermistors and an osmotic fluid sampler. Data were downloaded from Hole 1200C in March 2003. Pressure data used in this study are measured hourly with sensors at the seafloor and within the formation. Two pressure transients were seen in the data recorded on October 12, 2001 and March 26, 2002 that correspond to pressure responses to tectonic strain events. These pressure transients can be used to estimate regional hydraulic properties of the Mariana forearc which is difficult and expensive to access. Over the two year period that the CORK in Hole 1200C was recording, 39 body wave magnitude five or greater earthquakes occurred within a 500 km radius from the CORK location. The two largest earthquakes were moment magnitude 7.0 and correspond to both pressure transients. They will be referred to as EQ1 and EQ2.

CORK pressure data are processed and analyzed. The corrected data show that there is an initial pressure increase of 7.5 kilopascals (kPa) that occurs with EQ1 and 4 kPa that

occurs with EQ2. The pressure increase with EQ1 displays an estimated volumetric strain of 1.95×10^{-6} while the pressure increase with EQ2 has an estimated volumetric strain of 1.0×10^{-6}.These pressure increases occur at the same time as the two large earthquake events and are followed by a slow decay pressure. This decay is governed by the hydraulic properties of the formation and the long time period alludes to the hydraulic diffusivity of the formation. Literature suggests that this instantaneous response of pressures at the time of EQ1 and EQ2 as well as this slow decay of pressures are indicative of large scale contraction in which a large section of the plate contracts as slip occurs. It is proposed that two large contractions occurred within the Pacific plate or at the slab boundary, causing strain to build up at Hole 1200C at the time of both EQ1 and EQ2.

ACKNOWLEDGEMENTS

I would like to acknowledge the people who have been instrumental in my life and career as a geologist by guiding me to this point in my career. First I want to recognize my family and friends for their continued support. I have to thank my husband Carlos Vinas for his unconditional love and support and for being my rock throughout this whole process. I want to thank my parents Clifford and Janet Cooks for their love and words of wisdom. I must thank my sisters Kelia and Kimber Cooks for always being there for me. I also want to thank my mother and father-in-law for supporting Carlos and I while we lived in Miami. I need to thank my best friends Kristine Mills and Jasmine Langston for being true friends for so many years. I also want to thank my first geology professor Aditya Kar for inspiring me at such a young age. I cannot forget to thank my RSMAS friends Putri Akmal, Viviana Diaz, Kelly Jackson, and Andrew Jo for their kindness and support.

I also want to acknowledge my master's advisor Keir Becker for giving the opportunity to expand my education by accepting me into the University as a master's student and providing full support through a research assistantship. I would also like to thank my committee members Guoqing Lin and John Van Leer for agreeing to be a part of my committee and helping to guide me through the completion of my thesis through their critiques and thought provoking questions. I want to also thank the faculty and staff at the Rosenstiel School of Marine and Atmospheric Science for the advice, support and kind words that were offered to me. I have immensely enjoyed my time at the University of Miami and I will always look back on my time here with fond memories.

TABLE OF CONTENTS

LIST OF FIGURES

LIST OF TABLES

CHAPTER ONE

INTRODUCTION

1.1. General Overview

The area of interest for this study is the southern portion of the Mariana forearc. The forearc region of the Mariana trench is located within the Mariana convergent plate system that is found in the western Pacific Ocean (**Figure 1.1**). The Mariana trench and forearc are created by the convergence of the Pacific plate with the Philippine Sea plate beginning in the early Eocene (Fryer et al., 2006). Subduction is perpendicular to the trench at a rate of 35–45 mm/yr at 19N increasing to 55–70 mm/yr at 13.5N (Kato et al., 2003). As the older Jurassic Pacific plate subducts beneath the Philippine Sea plate an island arc and back arc basin is formed (Figure 1.2).The forearc crust, located between the trench and the island arc, is formed as a result of this collision and is non accretionary, meaning that it does not have the thick accumulation of marine sediments that is characteristic of many continental and island arc convergent margins. This exposure of the lithosphere and simple geology makes the Mariana convergent margin one of the most unique margins to study (Fryer, 1996).

1.2.Mariana Margin Seismicity

Seismicity in the southern Mariana subduction zone consists of swarms of shallowly dipping thrust earthquakes (Emry et al., 2011). There are few permanent seismic stations in the region so the majority of these earthquakes are detected teleseismically. The Mariana convergent margin is considered to be largely aseismic in comparison to very active margins like the Chilean and Alaskan convergent margins (Emry et al., 2011). Large M_w>8 earthquakes do not occur here very often. One widely accepted reason for

this is that the Mariana region is mostly seismically decoupled with no large interslab earthquakes occurring (Harada and Ishibashi, 2008).

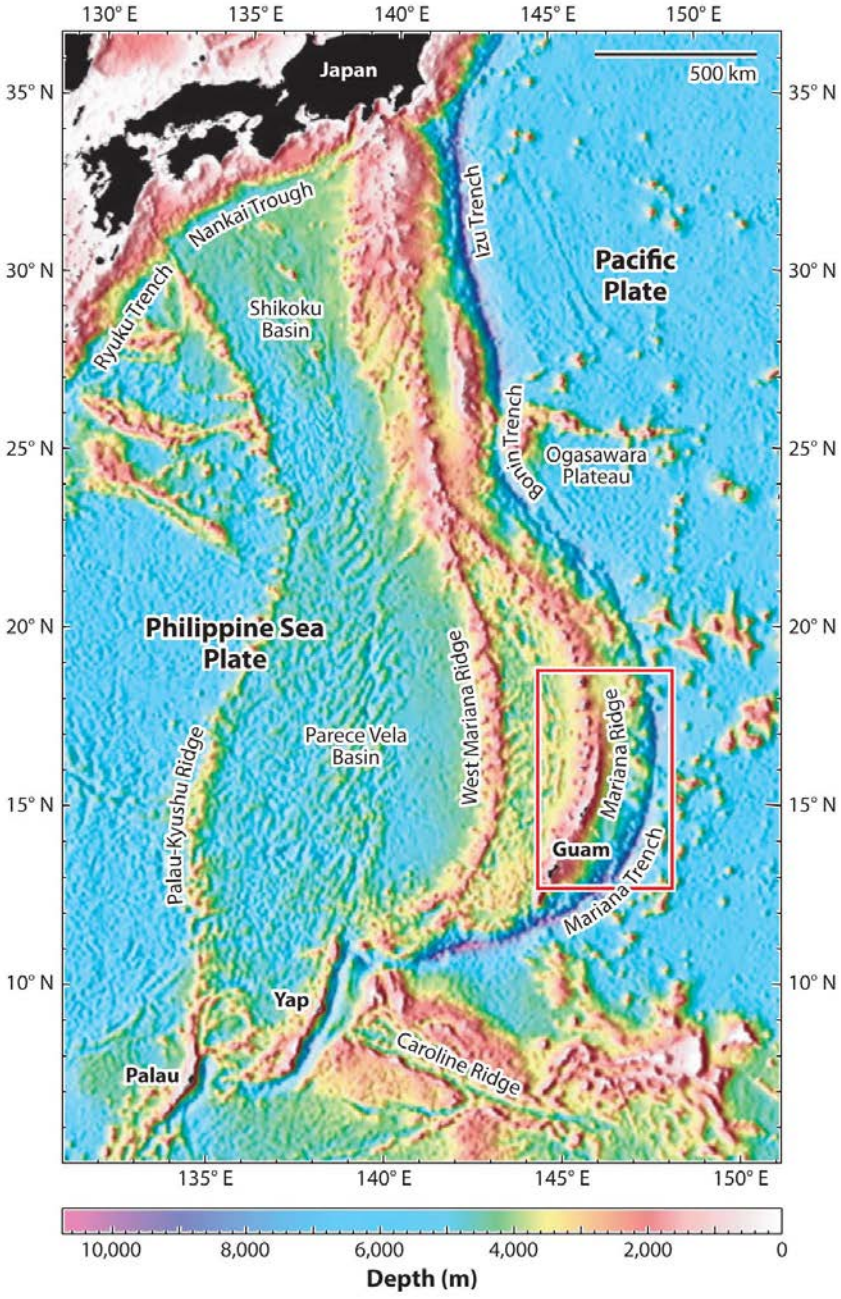

Figure 1.1: Color bathymetry regional overview map of the Mariana convergent margin. The southern Mariana forearc region is outlined in red and is also the position of figure 2.1. Modified from Fryer, 2012.

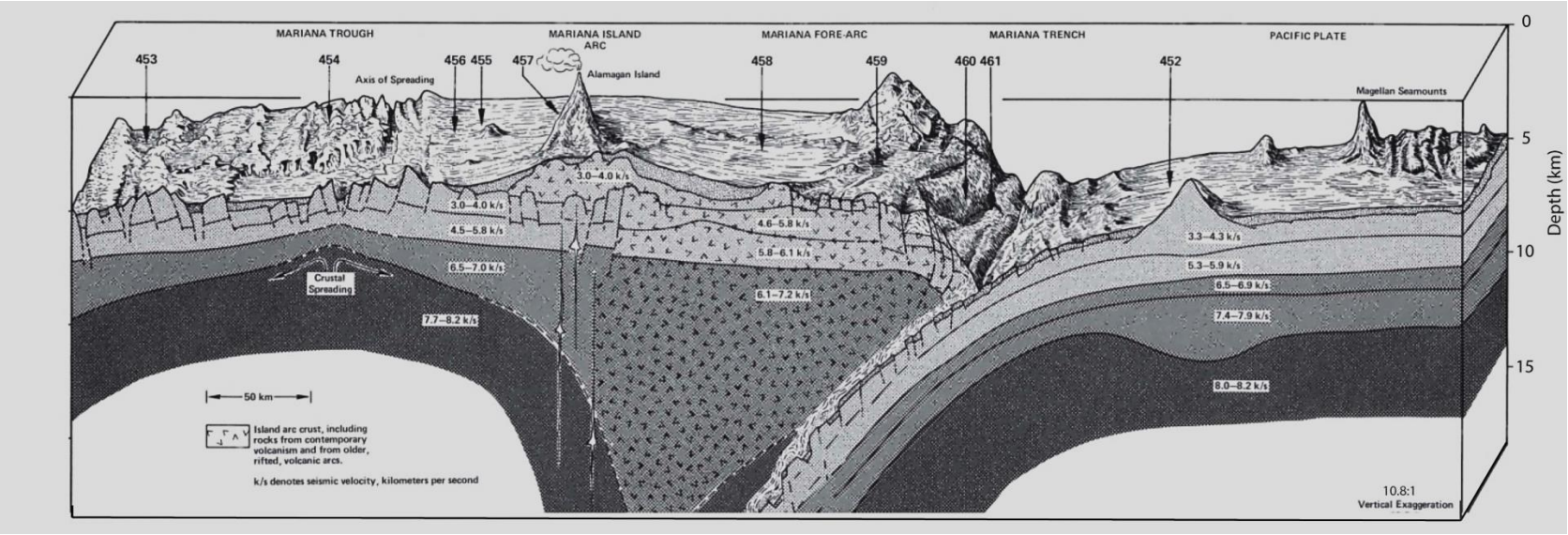

Figure 1.2: Schematic cross section of the Mariana convergent margin displaying the Pacific and Philippine Sea plate, and the locations of the trench, forearc, island arc, and trench. Modified from Fryer, 1996

CHAPTER TWO

BACKGROUND

2.1. Mariana Forearc Crust

The Mariana forearc crust is composed mostly of unconsolidated serpentine mud that contains clasts of serpentinized mantle peridotite (Shipboard Scientific Party Site 1200, 2002). This is one of the few areas where active blueschist mud volcanism, which provides valuable information about the composition of the fluids released from the subducting slab and the pressures and temperatures at (unreachable) depth in a subduction zone, has been observed (Shipboard Sci. Party Site 1200, 2002). The forearc is characterized by having many faults, created by a strongly extensional environment, exposing the crust and upper mantle lithosphere (Fryer, 1996). The faults in the forearc region serve as conduits for the rise of hydrated slab material which facilitates the formation of many large seamounts like South Chamorro seamount (Figure 2.1). The Mariana forearc crust is excellent for use in studies of subduction tectonics as the history of deformation and metamorphism is evident through sediment composition and seafloor mapping.

2.2. Ocean Drilling Program

For many of the reasons stated above, Site 1200 was chosen as a location to study during the Ocean Drilling Program Leg 195. The Ocean Drilling Program or ODP was a partnership created by an international joint effort whose purpose was to understand the "aspects of Earth's history, structure, and processes that can best and often only, be

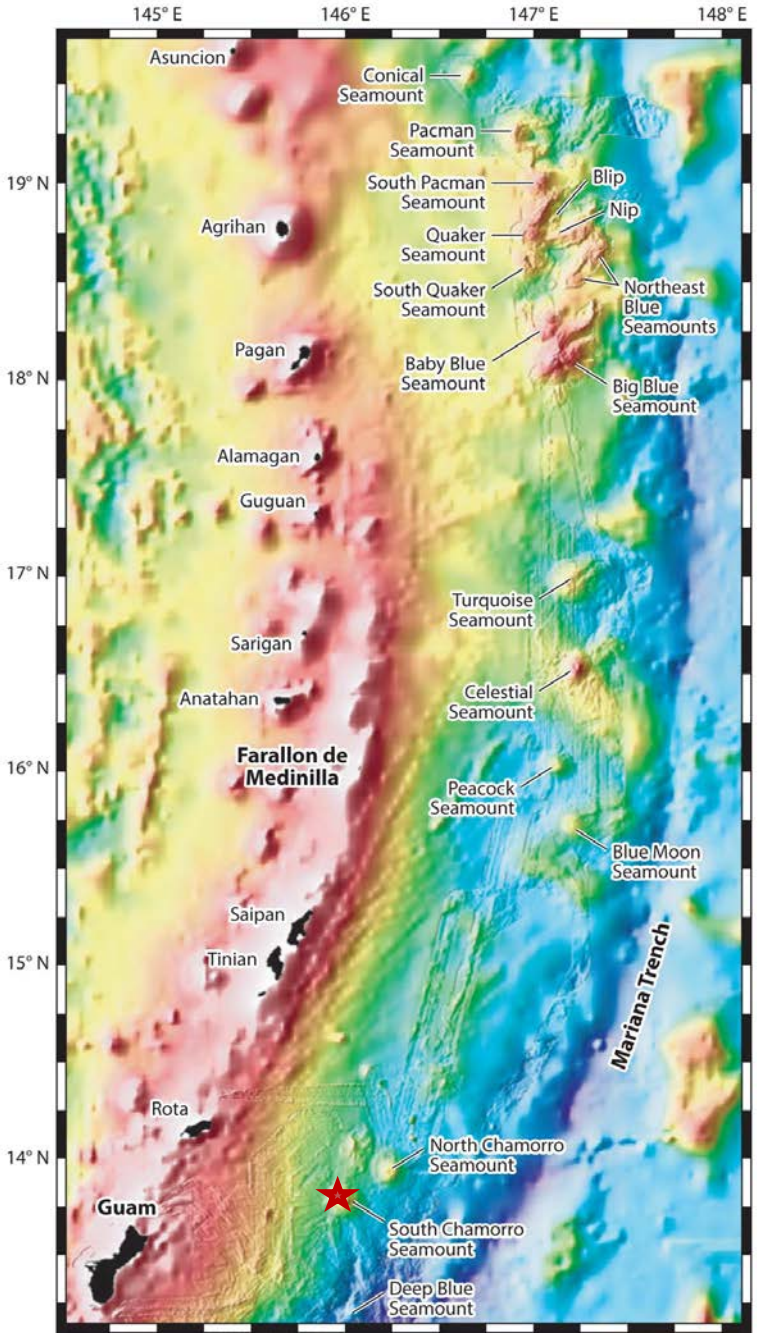

Figure 2.1: Color bathymetry map of the Mariana forearc crust showing the many seamounts present in the region. The location of South Chamorro seamount is highlighted with a red star. Modified from Fryer, 2012.

addressed by ocean drilling" (Joint Oceanographic Institutions, 1996). In 1989 the CORK program was initiated as a way to study ocean processes in situ as well as to stop the perturbation of hydrological systems due to the cased re-entry holes that existed after the Deep Sea Drilling Project (Becker and Davis, 2005). The CORKs are appropriately named Circulation Obviation Retrofit Kits after their designed purpose which is to stop the flow of fluids between the ocean and formation and to be borehole laboratories fitted with instrument kits.

2.3. ODP Leg 195, Site1200

The main goals of Leg 195 Site 1200 were to drill core samples and to place a long term borehole observatory at South Chamorro seamount in order to better understand the geochemical, biological, and geological processes that occur with subduction (Shipboard Scientific Party Site 1200, 2002). Holes 1200A-B and 1200D-F, located on the knoll of South Chamorro seamount, were cored either with a rotary core barrel or an advanced hydraulic piston corer. Due to stability issues Hole1200B was abandoned with no core recovery. Over 264 meters of core are recovered and analyzed.

The CORK at Site 1200, Hole 1200C is located on top of South Chamorro seamount about 85 KM away from the Mariana trench at 13°47′N, 146°00′E (**Figure 2.2**). It is located on a summit knoll about 200 m above the seafloor in a water depth of about 2910 m (Shipboard Scientific Party Site 1200, 2002). The surface of the knoll is broken into slabs of serpentine mud that are separated by shallow cross-cutting fissures. South Chamorro seamount is one of the many blueschist serpentine seamounts that exist in the Mariana forearc that are formed by hydrated slab materials coming up fractures in the crust creating mud volcanoes. An active biological community of mussels, gastropods

and other organisms feed off of the nutrients from low temperature springs that issue out of the fissures. This evidence supports that this seamount is still an active mud volcano.

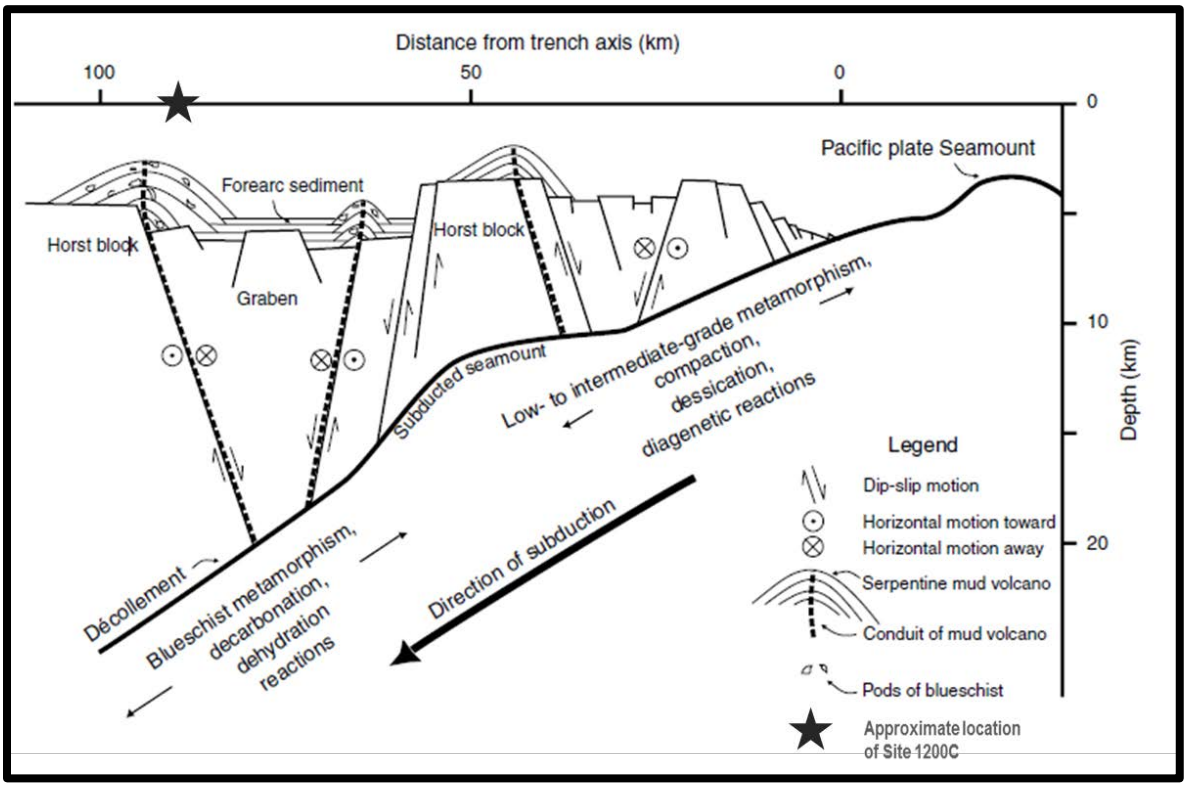

Figure 2.2: Schematic cross section of the Mariana trench and forearc showing the grabens, trench parallel lineations and large mud volcanoes that are composed of serpentine mud and serpentinize peridotite clasts. Site 1200C is located approximately 85 km from the trench axis. Figure modified from Shipboard Scientific Party Site 1200, 2002.

2.4. CORK Instrumentation, Installation, Data Download, and Removal

The borehole observatory at Hole 1200C was installed on March 14, 2001 during ODP Leg 195 with the *JOIDES Resolution* drillship. The borehole was drilled using a re-entry cone starting with 20-in casing and ending with 10.75-in casing. No core was recovered from 1200C during the drilling process. The hole was cased to a depth of 149 mbsf with the total depth of the hole being 266 mbsf. Attempts to drill deeper were

futile, therefore the hole was shorter than planned which created issues in the CORK instrument deployment. Screened casing was inserted from 149 mbsf to 202 mbsf leaving the remaining bottom portion of the hole open. The CORK assembly, which consisted of a thermistor cable, two pressure transducers at the seafloor and within the formation, two osmotic fluid samplers and a data logger, was then deployed in the hole (Shipboard Scientific Party Site 1200, 2002). The borehole was sealed at the top, creating a sealed borehole observatory (**Figure 2.3**).

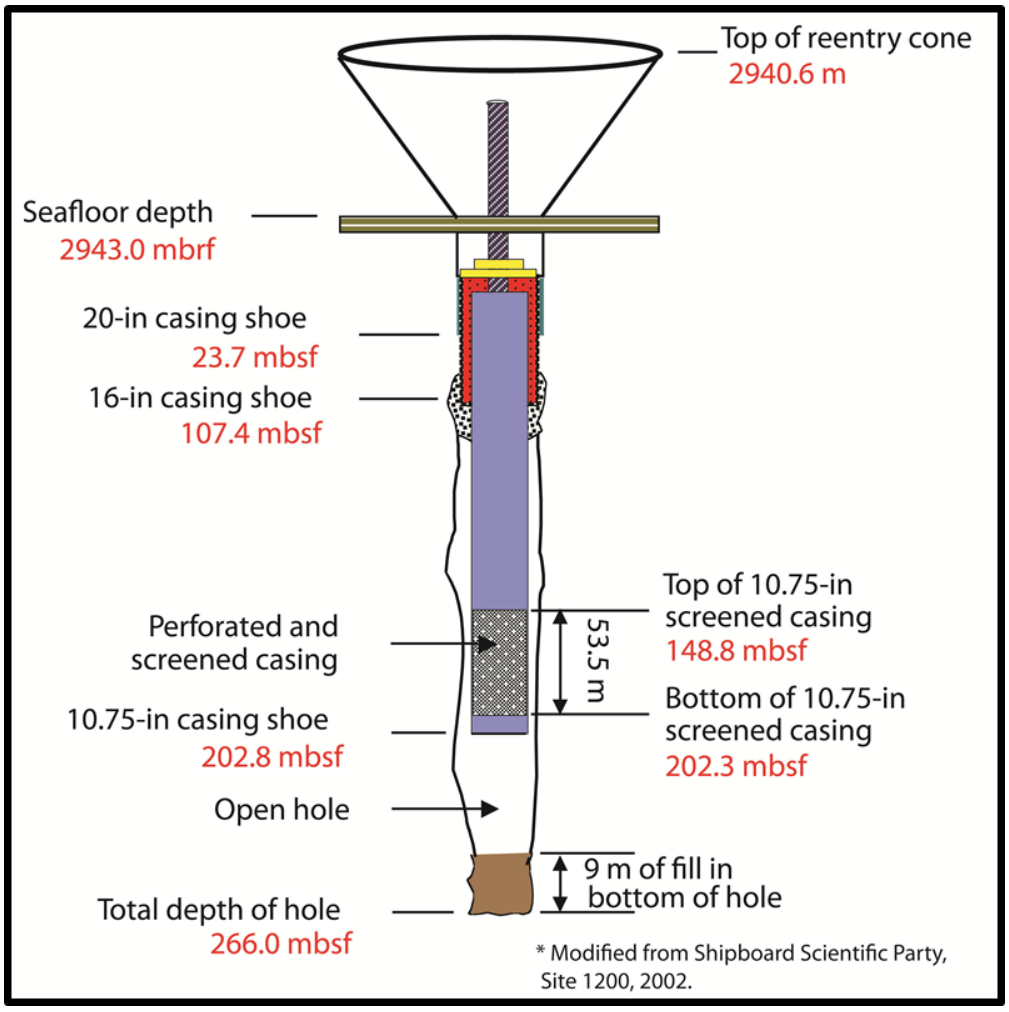

Figure 2.3: Schematic of the Circulation Obviation Retrofit Kit (CORK) in ODP Leg 195 Hole 1200C. Figure modified from Shipboard Scientific Party Site 1200, 2002**.**

On March 23, 2003 the CORK data were downloaded and the CORK sensor string was removed from the borehole with the remotely operated vehicle *Jason II*. Due to the shortening of the hole from the original plan, the thermistor string had to be shortened and was damaged as a result. Those temperature data are deemed unusable. The fluids in the osmotic fluid sampler were lost during the recovery of the sample tube. The tube burst as it was bought to the surface and the gasses within it became depressurized and expanded (Wheat et al., 2008). Pressure data remained intact with approximately two years of seafloor pressures and formation pressures recorded.

CHAPTER THREE

MOTIVATION

It is well known that subduction zones play a large role in recycling fluids between the ocean, lithosphere and mantle. As the down going slab subducts, its fluids are released into the mantle and back up through the forearc crust. Circulation obviation retrofit kits are a unique tool for studying these active processes in subduction zones. In situ measurements allow scientists to better understand what is happening in a particular setting without disturbing the natural processes. This is particularly important in deep sea low porosity settings that are difficult and expensive to access. Basic properties like permeability, compressibility, and loading efficiency that can be difficult to resolve in this highly faulted and fractured forearc crust are estimated using pressure data from CORKs. Pressure data from CORKs also record strain due to external forcing which are useful in understanding local tectonics. Calculations produced in this paper have many uses, particularly for estimating permeability using an elastic dislocation model or constraining permeability due to seafloor loading. Observations of the local tectonic environment along with pressure data can be helpful in understanding the relationship between strain and hydraulic properties of the formation.

CHAPTER FOUR

DATA

4.1. Raw CORK Pressure Data

Raw pressure data from Hole 1200C are downloaded and analyzed during this paper. At first glance the pressure data at the seafloor record nearly steady pressures at around 29747 kPa. The formation pressures, which are overpressured with respect to hydrostatic pressure, show that at day zero, formation pressures are perturbed from the drilling of the borehole. This allowed formation fluid to flow into the seawater and cold dense seawater to flow into the borehole causing the borehole pressures to decrease dramatically. Upon closer inspection it is evident that both formation and seafloor pressures are overprinted by periodic and aperiodic tidal, oceanographic and atmospheric signals. Spikes in the pressure signals at the seafloor and within the formation pressures are also observed. Two spikes or pressure changes occur at the seafloor, one on October, 12 2001 with a negative spike in pressure (although it is difficult to ascertain when the spike first occurs due to the one hour sampling period) and one on April 26, 2002 with a positive spike in pressure (**Figure 4.1**). These spikes must have occurred very close to the sampling time as we have an hourly sampling rate. There are also two pressure changes within the formation that occur concurrently with the spikes at the seafloor with both spikes being positive. The pressure increases that occur within the formation are sustained over time while the pressure increases at the seafloor do not appear to remain over time.

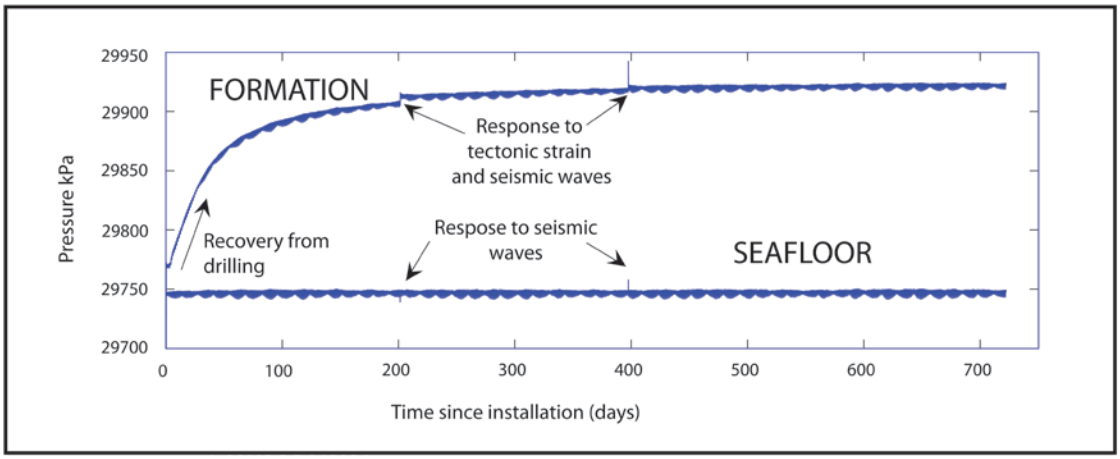

Figure 4.1: Plot showing raw seafloor and formation pressure signals changing with time. The formation pressures show the recovery of the pressures from drilling as well as two pressure transients caused by tectonic strain.

4.2. Earthquake Data

Over the two year period that the CORK in Hole 1200C was recording, 539 earthquakes occurred within a 500 km radius from the CORK location (**Figure 4.2**). These earthquakes ranged from a body wave magnitude (m_b) of 3 to 6.7 with an average m_b of 3.9 (ISC, 2011). Body wave magnitudes are used because moment magnitudes are not available for every earthquake. Earthquake events in this study were located using the International Seismological Centre (ISC) Database which contains a searchable catalog of earthquake data from seismic networks and data centers worldwide. The moment magnitudes of the two events highlighted in this paper were calculated using the global centroid moment tensor project catalog (GCMT). The GCMT project uses the centroid moment tensor algorithm to calculate and catalog earthquake focal mechanisms and magnitudes (Ekstrom, 2012). Fault plane solutions are from the National Earthquake Information Center (NEIC).

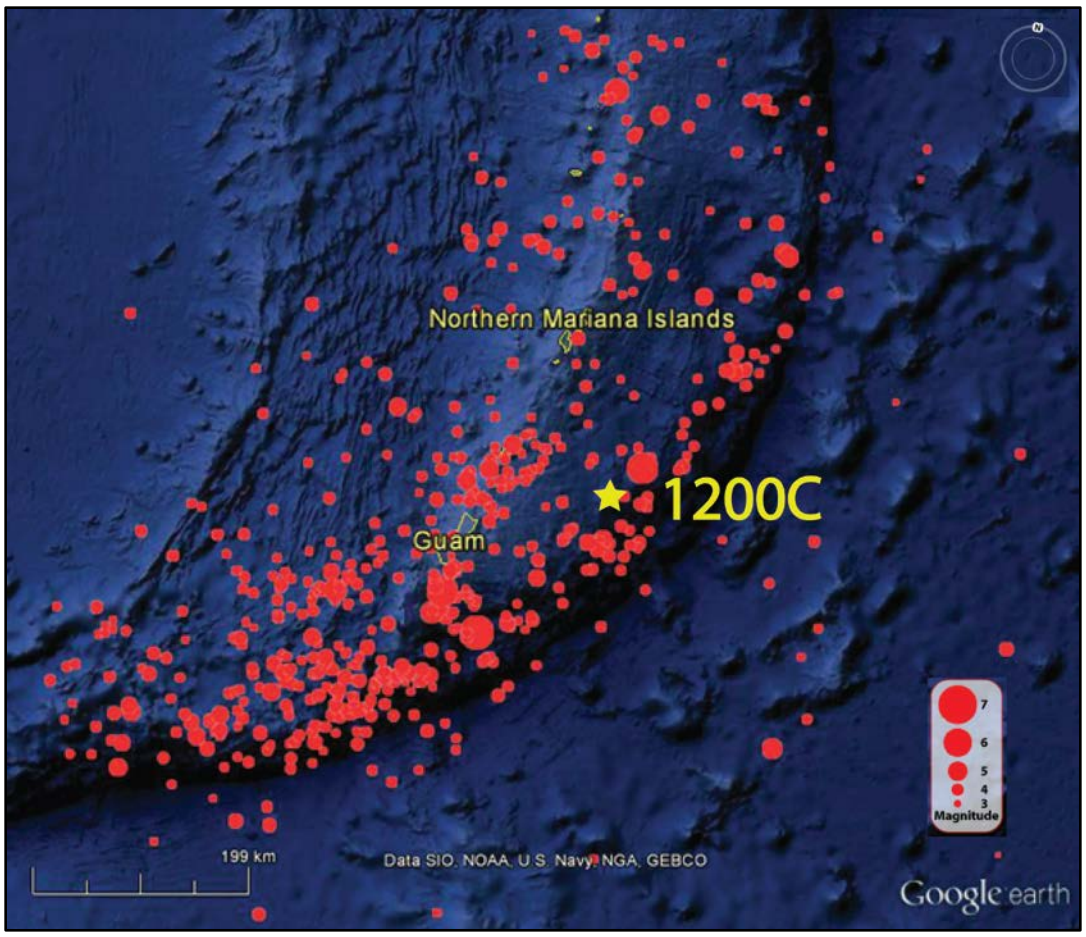

Figure 4.2: Map of all earthquakes that occurred during the two year time period that the CORK at Hole 1200C was deployed. Data are from the International Seismological Centre.

CHAPTER FIVE
METHODS

5.1. Removing Noise from Raw Pressure Data

CORK pressure data are strongly influenced by tidal, oceanographic and atmospheric effects. In order to identify any formation or seafloor pressure responses to tectonic strain events, these effects must first be removed. A tidal analysis package called Tidal Analysis Program in Python or TAPPy was used to remove these signals. TAPPy is written in Python which is a programming language used in scientific computing. Python has a free open source software library called SciPy which provides high level scientific tools that allow scientists to quickly and easily run programs. TAPPy uses SciPy's least squares optimization function to perform harmonic analysis of time series. This function allows the tidal components that overprint the pressure data to be broken down into individual sine waves and removed.

5.2. Using TAPPy to Remove Tides from Raw Pressure data

TAPPy is a very simple tool to use to perform harmonic analysis with pressure data. The first step requires creating a .txt file with data including dates and times of measurements and measured pressure values. Once the .txt file containing the data is created, the program calls for a data definition file used to define the variables needed to perform the analysis. This data definition file is a simple text document that tells the program where the data are in the file. After the files are created, TAPPy is run using Python. TAPPy analyses the pressure data by performing a harmonic analysis of the time series where the signal is broken down into component sine waves. Once TAPPy

completes the harmonic analysis of the time series, it outputs the tidal constituents measured from the frequencies found in the pressure data. TAPPy also outputs a file containing date and time information and cleaned pressure data with the tides removed.

5.3. Removing the Trend of Pressure Recovery from Drilling

Cleaned formation pressure data display a trend of pressures gradually increasing over time as the formation pressures are slowly returning to their unperturbed state after being disturbed due to the drilling and installation of Hole 1200C (**Figure 5.1**) . The cleaned formation pressures also display two spikes in the data, which correspond in time to two large earthquake events that have caused the formation pressures to quickly increase and slowly decrease over a period of months. The slow decrease of formation pressures after the earthquakes have occurred is of great interest to this study, and therefore must be isolated from the background increasing trend of increasing pressures. Isolating this trend is necessary to quantify the amount of pressure increase that occurred due to the earthquake alone and to better understand the length of time it takes for the pressures to return to their initial values.

Removing the background trend from the pressure data can be done in Microsoft excel using the trend line extrapolation function. Once pressure data are loaded into Excel and the increases due to the pressure perturbation are removed, an extrapolation can be done using control points. This creates a series of values that represent a first order approximation of the general shape of the curve excluding the pressure perturbations (**Figure 5.2**). Major assumptions are that the first pressure perturbation ends 40 days after the start of the second perturbation, and that the increase of pressure due to drilling stops around 500 days. These values are then subtracted from the original pressure data. The

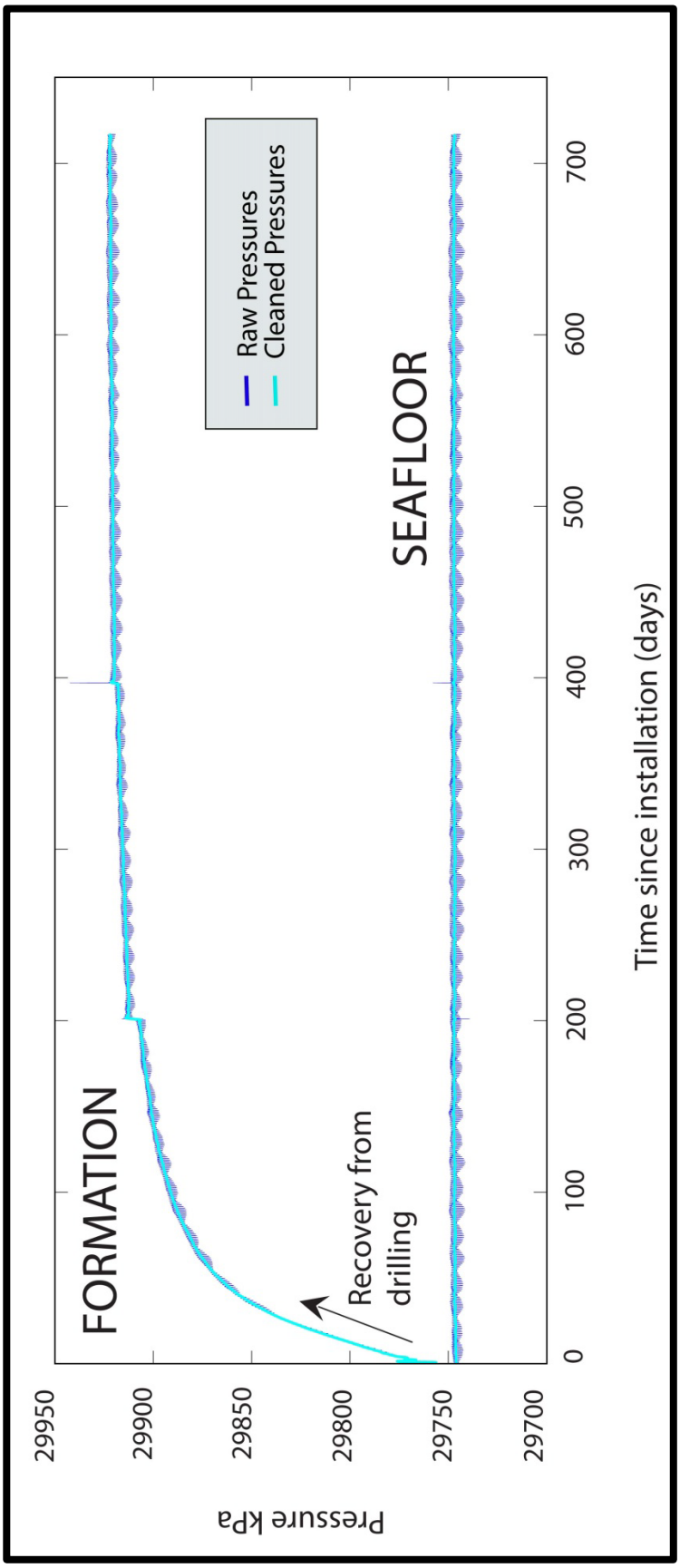

Figure 5.1: Pressure data used in this study with noise removed using the Tidal Analysis Program in Python (TAPPy) overlain on the raw pressure data.

resultant values should solely represent the pressure increases and slow decay of pressures due to the two earthquakes (**Figure 5.3**).

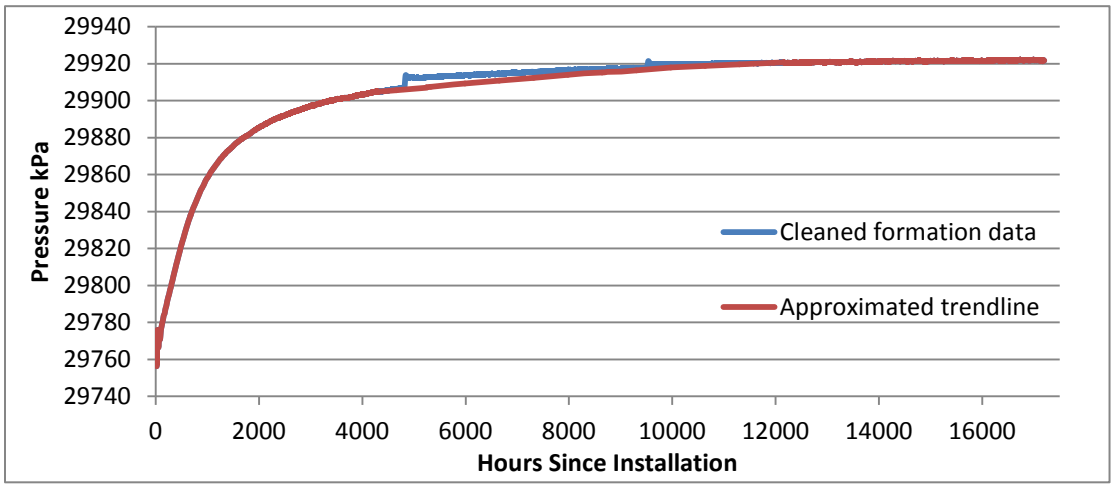

Figure 5.2: Plot showing cleaned formation pressures (blue) overlain by the approximated trend line (red) calculated using extrapolation.

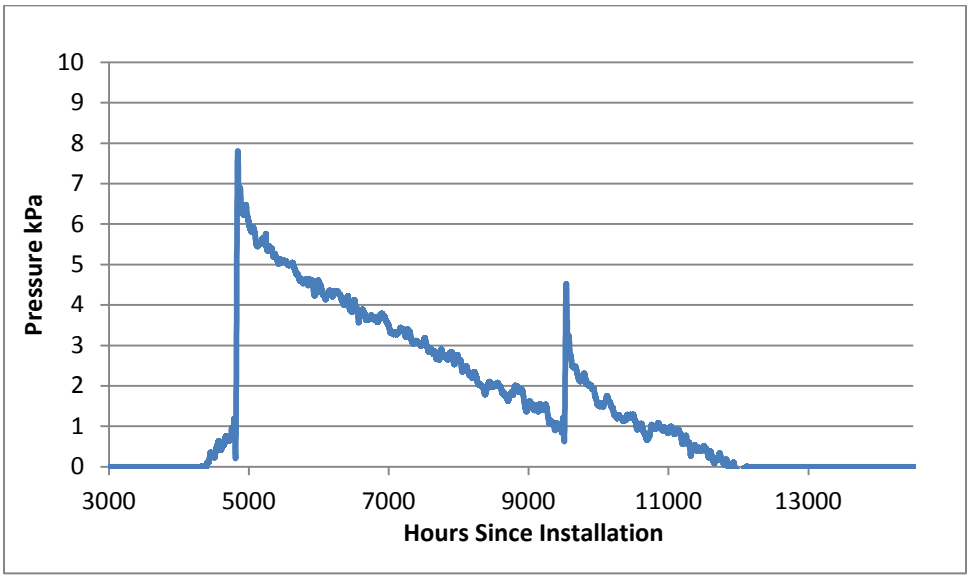

Figure 5.3: Plot showing isolated formation pressure data from the increase and slow decay of pressure due to the two earthquakes.

5.4. Calculation of Formation Properties

This study uses the following equations taken from Wang and Davis (1996) to calculate formation properties:

$$\beta = \alpha\left[\alpha + nK\left(\frac{1}{K_f} - \frac{1}{K_s}\right)\right]^{-1} \quad (1)$$

$$\alpha = 1 - \frac{K}{K_s} \quad (2)$$

$$\gamma = \frac{\beta(1+v)}{3(1-v)-2\alpha\beta(1-2v)} \quad (3)$$

where, β is the three-dimensional loading efficiency, α is expansibility, K is the bulk moduli of the matrix frame, K_f is the bulk modus of the fluid, K_s is bulk modulus of the solid constituents of the matrix, γ is the loading efficiency, v is Poisson's ratio and n is porosity. The values for these terms can be found in **Table 5.1**.

Each of these equations expresses how loads are divided between the matrix and the pore fluids based on their elastic properties- in particular compressibility. Equation one represents the three-dimensional loading efficiency of the rock or the compressibility of the formation. Loading efficiency is a number between zero and one that measures the partitioning of the vertical elastic stress between the pore fluid and the rock matrix (Wang and Davis, 1996; van der Kamp and Gale, 1983). Loading efficiency can be calculated from plugging in the values from equations1 and 2 into equation 3. A low loading efficiency is indicative of a more incompressible matrix while a higher loading efficiency is indicative of a more compressible matrix.

Calculating volumetric strain from pressure change was completed using the following equations taken from Davis and others (2001):

$$P = \beta\sigma_t \qquad (4)$$

$$\sigma_t - \alpha P = K\theta \qquad (5)$$

$$\theta = \frac{1-\alpha\beta}{\beta K} P \qquad (6)$$

where P is pore pressure increase, σ_t is the total pressure change and θ is volumetric strain. Pore pressure increase is expressed as equation 4 while β and α are defined by equations 1 and 2 respectfully. Effective pressure is related to volumetric strain by the relationship in equation 5. Under undrained conditions equation 6 computes the volumetric strain due to a given pressure change (Davis et al., 2001).

Parameter	Value	Source
K	6.52E+08 Pa	Akmal, 2013
K_f	2.40E+09 Pa	Davis et al., 2001
K_s	5.00E+10 Pa	Davis et al., 2001
v	0.31	Fryer et al., 2006b
n	0.45	Wheat et al., 2008
β	0.891	Calculated from equation 1
α	0.952	Calculated from equation 2
γ	0.8189	Calculated from equation 3
θ EQ1	1.9584E-06	Calculated from equation 6
θ EQ2	1.04448E-06	Calculated from equation 6

Table 5.1: Summary of parameters, values and their sources used for calculations in this study.

CHAPTER SIX
RESULTS

6.1. Earthquake Results

Earthquakes are sorted based on their magnitudes. 39 earthquakes with body wave magnitudes larger than 5.0 are mapped in relation to Hole 1200C and plotted on top of the formation pressure signal from Hole 1200C (**Figure 6.1 and 6.2**). The closest large earthquake to Hole 1200C occurred on August 14, 2002 and was about 39.6 km away with an M_w of 6.5. It was felt strongly on Guam and caused minor damages to some buildings on Saipan, (ISC, 2011). The closest earthquake occurred on August 11, 2001 about 35.4 km away from Hole 1200C with an m_b of 4.8 and depth 50.4 km. Of the 539 earthquakes that occurred two were close enough and large enough to affect the pore pressures at Hole 1200C. These earthquakes occurred on October 12, 2001 at 15:2:23.3 GMT and April 26, 2002 at 16:6:13.9 GMT and will be referred to as EQ1 and EQ2 respectively. EQ3 refers to the M_w 6.5 earthquake that occurred on August 14, 2002.

The two largest earthquake events correspond to the pressure spikes observed in the seafloor and formation pressure data from Hole 1200C. Both events were felt on both Guam and Saipan with EQ2 causing damage to infrastructure on Guam (ISC, 2011). The first event on October 12, 2001 was 165 km away from 1200C with a moment magnitude of 7.0 and a depth of 37 km (ISC, 2011). This event corresponds to a pressure increase within the formation at Hole 1200C and a negative spike in seafloor pressure. The second event on April 26, 2002 was 168 km away from 1200C with a moment magnitude of 7.0 and a depth of 85.7 km (ISC, 2011). This event corresponds to a pressure increase within

the formation and seafloor pressure at Hole 1200. Focal mechanisms for these events indicate that they are shallowly dipping thrust faults (**Figure 6.1**).

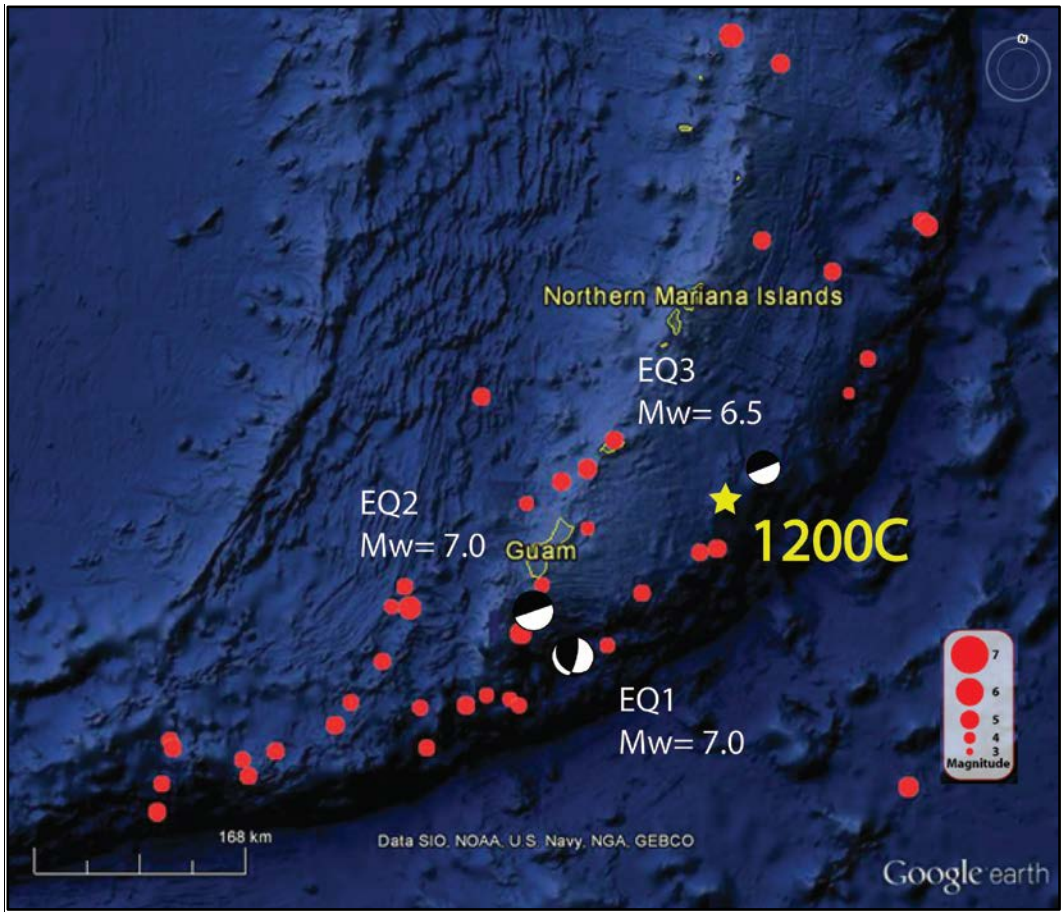

Figure 6.1: Map of all m_b ≥5 earthquakes at a 500 km radius around Hole 1200C during the time of CORK deployment. Focal mechanisms for the largest earthquakes are plotted. Data are from ISC, 2011.

6.2.Pressure Results

The isolated pressure data suggest that there is an initial pressure increase of 7.5 kPa that occurs with EQ1 and 4 kPa that occurs with EQ2. The pressure increase that occurs with EQ1 shows an initial increase in pressure followed by a slow decrease in pressure that lasts for about 245 days until it is cut off by the second pressure spike. The pressure increase that occurs with EQ2 shows an initial spike followed by a slow decay in

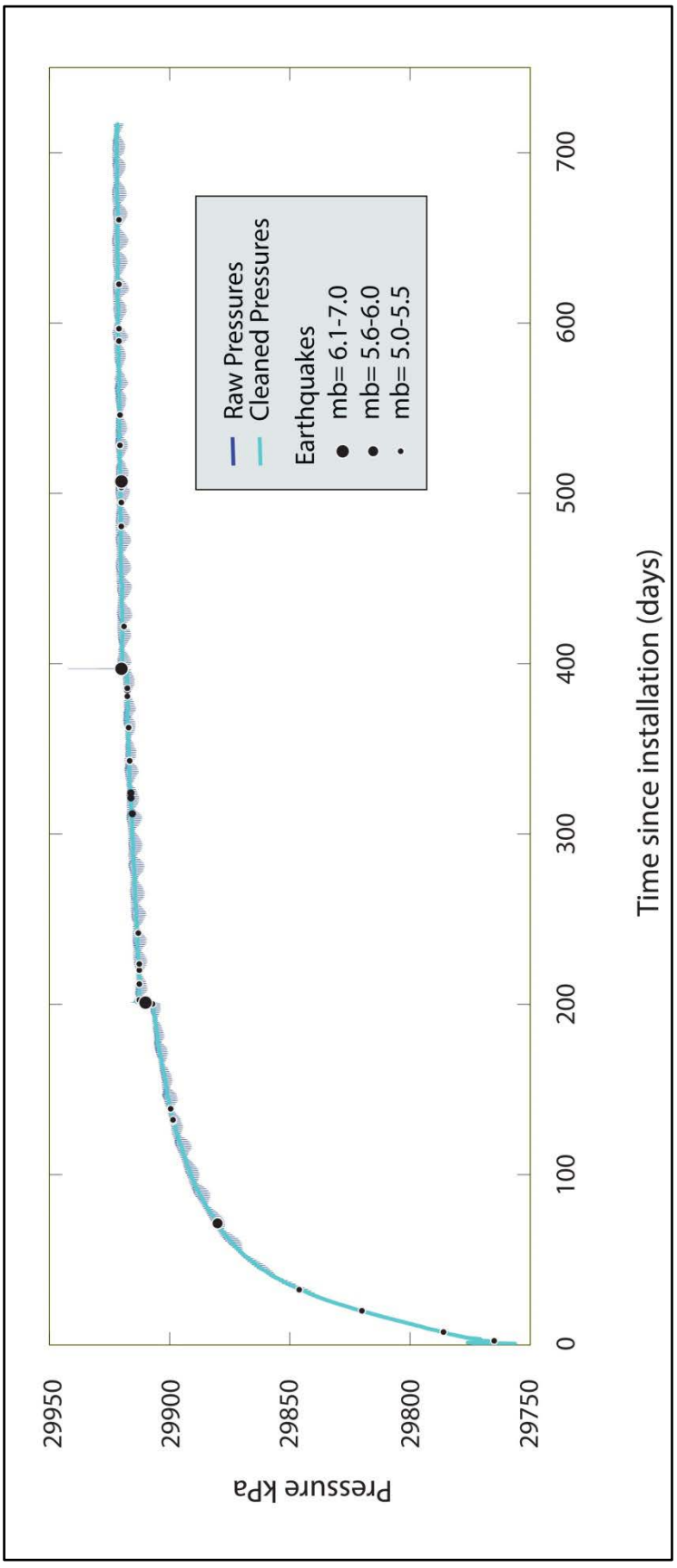

Figure 6.2: All body wave magnitude 5 and above earthquakes plotted on top of raw and cleaned formation pressure data.

pressures that takes about 104 days to return to the predicted initial pressure value that existed before the second pressure spike (**Figure 6.3**).

Date	Time	Lat	Lon	Mw	Mb	Ms	Depth km	Fault Plane 1			Fault Plane 2		
								Strike	Dip	Rake	Strike	Dip	Rake
10/12/2001	15:02:17	12.8600	144.9800	7	6.7	7.3	37	20	75	115	139	29	32
4/26/2002	16:06:07	13.0880	144.6190	7	6.5	6.8	85.7	60	80	90	240	10	90
8/14/2002	57:52.1	14.101	146.199	6.5	6.1	6.4	30	60	88	90	240	2	90

Table 6.1: Earthquake data for the three largest earthquakes that occurred during the deployment of the CORK in Hole 1200C. Taken from the International Seismological Centre.

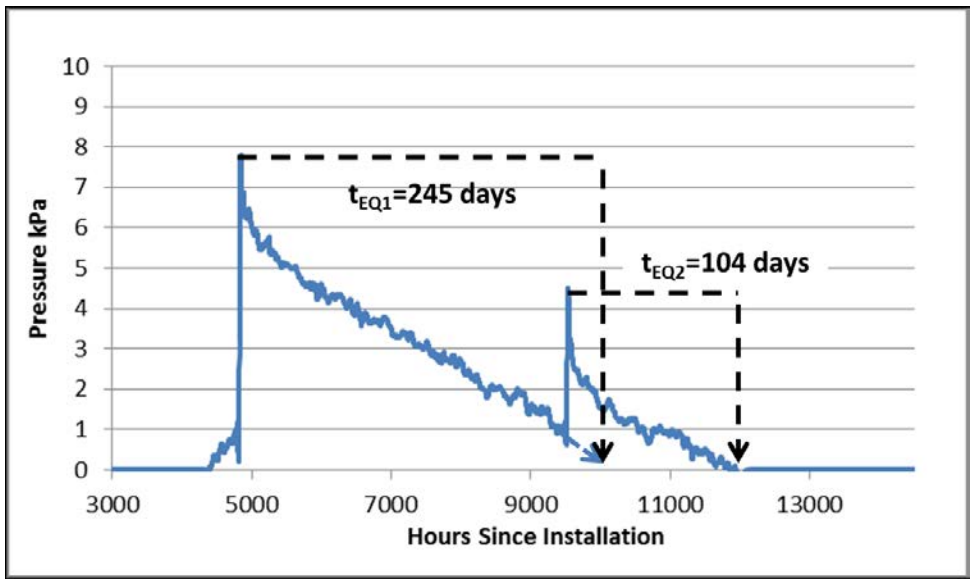

Figure 6.3: Isolated pressure data showing closer look at the two pressure anomalies and the time periods of pressure decay.

CHAPTER SEVEN

DISCUSSION

7.1. Implications from Timing of Earthquake Derived Pressure Anomalies

In the preceding sections we noted that the pressure anomalies following the two earthquake events took a significant amount of time to dissipate. The increase in pressure decays at rates that depend on the formation properties (Davis et al., 2004). The earthquakes are external forcing mechanisms that create pressure responses on a formation scale allowing formation properties like permeability to be resolved at a regional scale. There were several techniques used at or near Hole 1200C to calculate permeability but the heterogeneity in size of pore openings in the forearc crust as well as the difficulty of accessing the forearc crust for sub-seafloor testing make resolving permeability in the Mariana forearc crust difficult. The following section examines permeability values made in this area and gives information about the attempted permeability calculation performed in the early stages of this paper that uses the decay times of the earthquake derived pressure anomalies.

7.2. Permeability Values

The simplest way to obtain a measurement of permeability is to use cores taken from the formation of interest. In this method a core is drilled from the formation, cataloged and taken to a laboratory where physical properties are measured (Shipboard Scientific Party Site 1200C, 2002). A uniaxial floating-ring back-pressured consolidometer was used to measure the permeability of samples from Pacman Seamount, an ODP site close to Hole 1200C (Wheat et al., 2008). Measurements were taken at 25 degrees C with

vertical stresses varying from 25 to 3200 kPa. Permeability was measured at each pressure step using a "modified medical flow pump" that allows fluids to flow across the sample (Wheat et al., 2008). Next permeability was calculated by using Darcy's Law equations and measuring the pressure difference across each sample. Permeabilities measured at Pacman Seamount about 600 km away from South Chamorro Seamount range from 10^{-17} m^2 to $10^{-13}m^2$ depending on the rock types and porosity (Wheat et al., 2008). This method gives a first order small scale approximation of permeability due to the fact that only a small sample of the heterogeneous formation is tested. Measurements made at such a small scale in tight formations only represent permeabilities near the borehole and cannot account for the heterogeneity seen in highly fractured formations.

Another method for approximating the permeability of tight formations is the borehole outflow method. This method approximates permeability of a formation by estimating the rate of flow of formation fluid from an open borehole and applying a radial diffusion equation. The borehole outflow method was used in Hole 1200C when the CORK was removed and continuous fluid flow occurred from depth (Wheat et al., 2008). Given the rate of outflow over a specific time period, thickness of the open borehole, porosity, viscosity, and fluid compressibility, a radial diffusion equation can be used to calculate permeability (Fisher et al,. 1997). The permeability measured using this method at Hole 1200C was calculated to be 6 $x10^{-14}m^2$ (Wheat et al., 2008).This permeability represents a more regional value as it measures the permeability of the formation directly (meters) around the borehole and accounts for a larger portions of the heterogeneous pore sizes in the formation than the core method. This permeability is one order of magnitude greater than the average permeability measured in the forearc crust using core.

The tidal loading method uses the pressure response of the formation to loading created by oceanographic and atmospheric influences. Pressure responses from tidal, barometric and oceanographic forcing at the seafloor and within the formation are very well resolved using CORK data. Harmonic analysis of the pressure data gives the amplitudes and phases of the tidal frequencies. The amplitude and phase of the response to loading that occurs at the seafloor is generally not attenuated while the diffusive response from the seafloor to the formation is attenuated depending on the loading efficiency of the formation or the degree of which loads are delivered to the interstitial water. This attenuation or phase lag depends on the hydraulic diffusivity of the formation and is used in the calculation of permeability (Wang and Davis, 1996). The permeability value calculated at Hole 1200C by Akmal, 2013 is 2.76×10^{-13} m^2. This permeability is one order of magnitude greater than the permeability calculated by the borehole outflow method.

The final method that we attempted to use to calculate permeability in this study is analogous to the modified slug test method. During a slug test, a volume of fluid is injected in one location and the change in head is monitored in the source well or at another location. After the initial change in head due to fluid injection and pressurization, the head will decay as the pressures stabilize. This decay will occur at time periods that can be directly related to the hydraulic properties of the formation (Bredehoeft and Papadopulos, 1980). In this case, the earthquake pressure pulse represents the injection of fluid and 1200C is our observation well. The strain perturbation that occurs with an earthquake creates an increase in strain that is laterally transferred as a pressure pulse throughout the elastic medium to Hole 1200C causing, in this instance, an increase in the

pressure at 1200C. This pressure increase then reaches a peak and decays at rates that depend on the formation properties (Davis et al., 2004). This method is not valid for this data set due to the inconsistency between the large distance of the earthquake injection and the very short time period of the maximum pressure increase. At such large distances, the borehole pressures are expected to take a longer time, on the order of days, to reach the peak pressure value after being perturbed by the earthquake pressure pulse (Davis et al., 2004). An elastic dislocation model must be computed in order to understand the distribution of the strain due to the earthquake (Davis et al., 2001), which is beyond the scope of this paper.

7.3. Comparison of Strains Felt from Both Earthquakes

EQ1 and EQ2 were both M_w 7 earthquakes that occurred southwest of Hole 1200C around 165 km away from South Chamorro seamount. Although these two earthquakes are extremely similar in many respects, they each have different effects on the pressure signals at Hole 1200C. EQ1 displays a larger pressure increase of 7.5 kPa with an estimated volumetric strain of 1.958×10^{-6} while EQ2 has a smaller pressure increase of 4 kPa with an estimated volumetric strain of 1.044×10^{-6}. This may be partly due to poor sampling of the second pressure pulse. There was a large spike representing one data point that may account for a larger pressure increase during EQ2. This spike was removed during the de-tiding process. The distinct difference between the two earthquakes is their focal mechanisms. EQ1 has a more oblique thrust focal mechanism while EQ2 has a shallowly dipping thrust fault plane solution that is more common for the area. Another explanation for the differences in volumetric strains involves the distance and directivity effects of strain (Cotton and Coutant, 1997). EQ1 may be

preferentially oriented to deliver a larger amount of strain to the CORK at 1200C. This same reasoning could perhaps be used to explain the lack of pressure perturbations caused by the two closest earthquakes. This hypothesis can be tested using an elastic dislocation model.

7.4. Interplate vs. Intraplate Earthquakes

Literature (Uyeda and Kanamori, 1979; Scholz and Campos, 1995; Harada and Ishibashi, 2008) on the Mariana convergent margin suggests that the area is slab decoupled with no large slab boundary earthquakes occurring. Harada and Ishibashi, 2008 completed a relocation of EQ1 and EQ2 as well as a large M_w 7.8 earthquake that occurred in 1993. Using background earthquakes to determine the shape of the slab, they found that the three large earthquakes were located within the slab and not at the slab boundary. Data from this study support that the slab is decoupled as EQ1 and EQ2, two of the largest earthquakes that have occurred within a ten year time frame, occur within the forearc, at a depth of 37 km and 85.7 km. These depths are more consistent with a location deep within the slab and not at the slab interface (Harada and Ishibashi, 2008). The lack of aftershocks for these moment magnitude 7 earthquakes also supports this finding as large interslab earthquakes usually produce significant aftershocks (Harada and Ishibashi, 2008).

7.5. Strain Observations

Seafloor and formation pressure data from Hole 1200C show that the maximum pressure spikes take place simultaneously with the occurrence of the two earthquakes. The instantaneous response suggests that there is a large scale contraction occurring that affects the formation surrounding Hole 1200C and the area around 165 km away where

the two large earthquakes occur. This is indicative of large scale plate contraction where the plate elastically contracts as slip occurs (Davis et al., 2006). This phenomenon has been documented to occur in other tectonic settings. Davis et al. (2001) model coseismic and aseismic pressure increases and decreases in CORK borehole observatories in the Northern Juan de Fuca ridge. They found that the earthquakes were only aftershocks of a much larger aseismic spreading event on a segment of the ridge that affected CORK borehole pressures kilometers away. Davis et al. (2006) use CORKs to model a series of very low frequency earthquakes that occur in response to aseismic slip along the decollment in the Nankai subduction zone. Pressure increases and calculated volumetric strains in the three advanced CORKs suggest that this aseismic slip released a large amount of accumulated strain (Davis et al, 2006).

We propose that large scale contraction occurs here that is bought on by large rupture events within the subducting slab or at the slab boundary. The strain due to these rupture events is not all created by seismic rupture, there is likely an aseismic component. We propose a model that is analogous to the elastic rebound theory where slip occurs on a fault releasing the stress at the fault, but creating strain along other portions of the fault slip zone. A large contraction occurred at the time of EQ1 and EQ2 from slip that occurred either within the Pacific plate or at the slab boundary, causing strain to build up at Hole 1200C and at locations of EQ1 and EQ2 (**Figure 7.1**). This model fits well for this convergent margin in that slip is largely aseismic. This could also explain the lack of pressure perturbations occurring with EQ3 and other earthquakes as they may not be associated with a larger aseismic event.

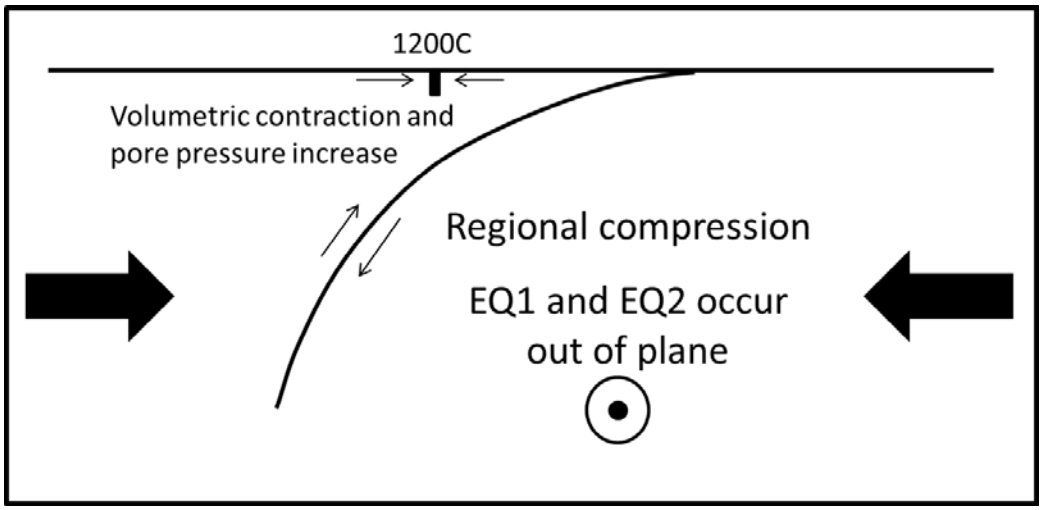

Figure 7.1: Schematic figure depicting regional compression that occurs at the time of EQ1 and EQ2 causing pore pressures to increase at Hole 1200C.

CHAPTER EIGHT

CONCLUSION

The Mariana forearc crust is a unique location to study, as it is the end member example of a non-accretionary aseismic subduction zone. Circulation Obviation Retrofit Kits (CORKs) provide a way to understand active processes that occur here in situ without continued disruption of the natural environment. Formation pressure data from the CORK in Hole 1200C show a record that is dominated by tidal influences with a slightly increasing trend due to the perturbation of the borehole pressures from drilling. Two pressure increases of 7.5 kPa and 3.5 kPa are also documented that occur nearly simultaneously with two moment magnitude 7.0 earthquakes. The instantaneous response of the pressure increases occurring with the earthquake events make these data unsuitable to use to calculate permeability using the model analogous to a modified slug test. Instead permeability must be calculated using an elastic dislocation model. The instantaneous response followed by a slow decay in pressure suggests that there is a large scale contraction occurring with the two earthquakes causing the two pressure perturbations. This model fits with the largely aseismic convergent margin.

REFERENCES

Becker, K and E. Davis, 2005. A review of CORK designs and operations during the Ocean Drilling Program. In Fisher, A.T., Urabe, T., Klaus, A., and the Expedition 301 Scientists, Proc. IODP., 301: College Station, TX (Ocean Drilling Program), 1-28.

Bredehoeft, J. D. and S. S. Papadopulos, 1980. A method for determining the hydraulic properties of tight formations. *Water Resources Research* **16**(1): 233-238.

Cotton, F. and O. Coutant, 1997. Dynamic stress variations due to shear faults in a plane-layered medium. *Geophys. J. Int*. **128**, 676-688.

Davis, E.E., Wang, K., Thompson, R.E., Becker, K., and Cassidy, J.F., 2001. An episode of seafloor spreading and associated plate deformation inferred from crustal fluid pressure transients. *J. Geophys. Res*. **106**:21, 953-963.

Davis, E.E., Becker, K., Dziak, R., Cassidy, J., Wang, K., and Lilley, W., 2004. Hydrological response to a seafloor spreading episode on the Juan de Fuca ridge. *Nature*. **430**, 335-338.

Davis, E. E., Becker K., Wang K., Obara K., Ito Y., and Kinoshita M., 2006. A discrete episode of seismic and aseismic deformation of the Nankai trough subduction zone accretionary prism and incoming Philippine Sea plate, *Earth Planet. Sci. Lett.* **242**, 73–84.

Ekström, G., Nettles, M., and Dziewoński, A.M., 2012. The global CMT project 2004–2010: Centroid-moment tensors for 13,017 earthquakes, *Physics of the Earth and Planetary Interiors* **200**, 1-9.

Emry, E. L., Wiens, D. A., Shiobara, H., and Sugioka, H., 2011. Seismogenic characteristics of the Northern Mariana shallow thrust zone from local array data, *Geochem. Geophys. Geosys.* **12**, 1-25.

Fryer, P., 1996. Tectonic evolution of the Mariana convergent margin, *Rev. Geophys.* **34**, 89–125.

Fryer, P., Gharib, J., Ross, K., Savov, I., Mottl, M., 2006. Variability in serpentine mudflow mechanisms and sources: ODP drilling results on Mariana forearc seamounts, *Geochem. Geophys. Geosyst.,* **7**:8, 1-15.

Fryer, P.B., and M.H Salisbury, 2006. Leg 195 synthesis: Site 1200—serpentinite seamounts of the Izu-Bonin/Mariana convergent plate margin (ODP Leg 125 and 195 drilling results). *In* Shinohara, M., Salisbury, M.H., and Richter, C. (Eds.), *Proc. ODP, Sci. Results,* 195: College Station TX (Ocean Drilling Program), 1–30.

Fryer, P., 2012. Serpentinite Mud Volcanism: Observations, Processes, and Implications. *Annual Review of Marine Science,* Vol 4. C. A. Carlson and S. J. Giovannoni. Palo Alto, Annual Reviews. **4**, 345-373.

Harada T. and K. Ishibashi, 2008. Interpretation of the 1993, 2001, and 2002 Guam earthquakes as intraslab events by a simultaneous relocation of the mainshocks, aftershocks, and background earthquakes, *Bull. Seism. Soc. Am*. **98**:3, 1581-1587.

International Seismological Centre, *On-line Bulletin*, http://www.isc.ac.uk, Internet. Seis. Cent., Thatcham, United Kingdom, 2011.

Joint Oceanographic Institutions, 1996. Understanding our dynamic earth through ocean drilling: Ocean drilling program long range plan into the 21st century first ed., Vol. 1, pp. 1-79. Joint Oceanographic Institutions, Washington, DC.

Kato, T., Beavan, J., Matsushima, T., Kotake, Y., Camacho, J., and Nakao, S., 2003. Geodetic evidence of back-arc spreading in the Mariana Trough, *Geophys. Res. Lett*. **30:**12, 1-4.

Scholz, C.H., and J. Campos, 1995. On the mechanism of seismic decoupling and back-arc spreading at subduction zones, *J. Geophys. Res.* **100**:22, 103-115.

Shipboard Scientific Party, 1990. Site 778. In Fryer, P., Pierce, J. A., Stokking, L. B., et al*., Proc. ODP, Init. Repts*., 125: College Station, TX (Ocean Drilling Program), 97-114.

Shipboard Scientific Party, 2002. Leg 195 summary. In Salisbury, M.H., Shinohara, M., Richter, C. *Proc. ODP, Init. Repts*., 195: College Station, TX (Ocean Drilling Program), 1-63.

Uyeda, S., and H. Kanamori, 1979. Back-arc opening and the mode of subduction, *J. Geophys. Res*. **84**, 1049–1061.

Wheat, G.C., Fryer, P., Fisher, A.T., Hulme, S., Jannasch, H., Mottl, M.J., Becker, K. 2008. Borehole observations of fluid flow from the South Chamorro Seamount an active serpentine and mud volcano in the Mariana Forearc. *Earth and Planetary Sci. Lett.* **267**:401-409.

APPENDIX

This table contains a list of all body wave magnitude 5 and up earthquakes that occurred during the length of the CORK deployment. Data were taken from the International Seismological Centre.

DATE	TIME	LAT	LON	DEPTH	AUTHOR	TYPE	MAG
3/29/2001	2:01:24	12.636	143.643	33.7	NEIC	m_b	5
4/2/2001	6:50:04	11.845	147.385	33	HRVD	M_w	5.5
4/14/2001	19:16:14	12.863	144.609	30.7	HRVD	M_w	5.3
4/27/2001	18:58:46	15.727	147.442	35.2	HRVD	M_w	5.3
6/4/2001	22:41:05	17.015	145.999	107.3	HRVD	M_w	5.7
8/3/2001	22:13:01	11.802	142.717	21.8	NEIC	m_b	5
8/4/2001	18:55:10	15.757	147.404	50.1	HRVD	M_w	5.1
8/11/2001	5:26:02	13.475	145.97	50	ISC	m_b	5
10/11/2001	21:06:55	11.97	142.17	54.2	NEIC	m_b	5.1
10/12/2001	15:02:20	12.716	144.975	61.8	HRVD	M_w	7
10/14/2001	5:02:57	12.347	143.429	33	HRVD	M_w	5.2
10/23/2001	12:04:53	14.197	145.223	97.1	NEIC	m_b	5.1
10/31/2001	19:12:13	14.797	147.014	24.8	MOS	m_b	5
11/4/2001	8:33:40	15.392	146.749	40.6	BJI	m_b	5
11/22/2001	11:18:33	11.913	142.671	33	MOS	m_b	5
1/31/2002	10:05:04	15.594	146.242	62.2	BJI	m_b	5.1
2/9/2002	18:27:01	13.749	144.622	155.1	BJI	m_b	5.2
2/12/2002	15:39:56	13.905	144.861	134.8	HRVD	M_w	5.8
3/3/2002	11:52:32	13.015	143.695	140.1	BJI	m_b	5.1
3/23/2002	3:06:16	11.983	142.907	17.2	HRVD	M_w	5.2
4/10/2002	11:47:23	11.515	142.068	36.7	ISC	M_S	5
4/14/2002	5:58:34	14.466	144.282	411.8	BJI	m_b	5.1
4/15/2002	3:52:07	13.011	143.823	121.2	HRVD	M_w	5.4
4/26/2002	16:06:05	13.032	144.688	69.1	HRVD	M_w	7
5/21/2002	23:45:34	13.998	145.04	131.4	HRVD	M_w	5.2
7/19/2002	3:37:54	12.185	143.323	47.4	HRVD	M_w	5.1
8/2/2002	6:32:45	16.829	146.359	64	HRVD	M_w	5
8/11/2002	0:59:13	13.159	145.448	62.2	BJI	m_b	5
8/14/2002	13:57:55	14.036	146.278	54.5	HRVD	M_w	6.5
9/4/2002	19:40:38	13.198	144.748	53.7	BJI	m_b	5
9/22/2002	16:33:55	12.795	145.216	43.4	MOS	m_b	5.1
11/5/2002	1:32:01	11.7137	142.0969	44.2	MOS	m_b	5.1
11/12/2002	7:12:40	13.5941	145.0543	128.8	HRVD	M_w	5.3
12/8/2002	8:16:50	12.3545	144.2381	34.7	HRVD	M_w	5.1

12/8/2002	11:29:09	12.4297	144.3798	33	BJI	MS	5.4
12/8/2002	14:47:40	12.3666	144.6107	57.7	MOS	m_b	5.1